nature structural & molecular biology

Biological basis for restriction of microRNA targets to the 3′ untranslated region in mammalian mRNAs

Shuo Gu[1], Lan Jin[1], Feijie Zhang[1], Peter Sarnow[2] & Mark A Kay[1]

MicroRNAs (miRNAs) interact with target sites located in the 3′ untranslated regions (3′ UTRs) of mRNAs to downregulate their expression when the appropriate miRNA is bound to target mRNA. To establish the functional importance of target-site localization in the 3′ UTR, we modified the stop codon to extend the coding region of the transgene reporter through the miRNA target sequence. As a result, the miRNAs lost their ability to inhibit translation but retained their ability to function as small interfering RNAs in mammalian cells in culture and *in vivo*. The addition of rare but not optimal codons upstream of the extended opening reading frame (ORF) made the miRNA target site more accessible and restored miRNA-induced translational knockdown. Taken together, these results suggest that active translation impedes miRNA-programmed RISC association with target mRNAs and support a mechanistic explanation for the localization of most miRNA target sites in noncoding regions of mRNAs in mammals.

miRNAs are a class of short, 20–22-nt regulatory RNAs expressed in plants and animals[1,2]. Up to 4% of the human genome is predicted to code for more than 400 miRNAs, which are estimated to regulate at least 30% of all human genes[3–5]. Although the specific functions of very few have been well established, a growing body of evidence indicates that miRNAs have important regulatory roles in a vast range of biological processes[6–8]. In plants, most miRNAs hybridize to target mRNAs with a near-perfect complementarity, and they mediate an endonucleolytic cleavage through a similar, if not identical, mechanism to that used by the small interfering RNA (siRNA) pathway[9]. In animals, with few exceptions, most of the known miRNAs form an imperfect duplex, with sequences located solely in the 3′ UTR region of target mRNA (base-pairing of a minimum 7-nucleotide seed sequence is required)[10–12]. The central mismatch between miRNA-mRNA hybridization may be responsible for the lack of RNAi-mediated mRNA-cleavage events in animals[13,14]. The association between the miRNA-programmed RNA-induced silencing complex (RISC) and the target mRNA induces translational repression through a poorly understood mechanism. There is evidence supporting models in which translation repression occurs at the initiation stage or later steps, including elongation (reviewed in refs. 15,16). Repressed mRNA and associated Argonaute (Ago) proteins are enriched in Processing bodies (P-bodies), where endogenous cellular mRNAs are kept for storage and degradation[17,18], which may partially explain why miRNA-mediated translational inhibition is often coupled with some RISC-independent target-mRNA degradation[19].

In contrast to an siRNA, which can target almost any part of an mRNA and be fully functional, almost all identified target sites for endogenous miRNAs are located in the 3′ UTR of target mRNAs in animals. This has been established by extensive bioinformatic sequence analyses and by experimental approaches[2]. To further define the molecular events involved in miRNA-induced silencing, we cloned both the human mir-30 and *Drosophila melanogaster* bantam miRNA target sites into the 3′ UTR of the luciferase and green fluorescent protein (GFP) reporter genes so that, by deleting one nucleotide in the stop codon, we were able to extend the ORF into the target site while maintaining the bioactivity of the protein. Using these reporter constructs as a starting point, in combination with the corresponding short hairpin RNA (shRNA) and miRNA expression cassettes, we provide experimental proof that there is a functional basis for the observed distribution of miRNA target sites in mammalian systems.

RESULTS

miRNA-mediated repression is abolished in extended ORFs

To establish whether miRNAs can retain their negative regulatory activity if their targets remain in the 3′ UTR of an mRNA but become embedded within the coding sequence, we constructed luciferase expression plasmids that contained either (i) no miRNA target sites, (ii) tandem mir-30 target sites in the 3′ UTR or (iii) mir-30 target sites with an additional single-base insertion, abolishing the stop codon and extending the ORF through the mir-30 sites (**Fig. 1a**). Each plasmid was tested for miRNA-induced silencing in mammalian cells. Specifically, luciferase plasmids were co-transfected with plasmids that can direct the expression of miRNAs, such as sh-mir-30 (mismatch), sh-mir-30P (perfect complementarity) or sh-Scramble (scrambled control) (**Fig. 1b,c**).

We first established that the mir-30 and mir-30P expressed from U6-driven cassettes were processed correctly and resulted in similar levels

[1]The Center for Clinical Science Research, Room 2105, 269 Campus Drive, Stanford, California 94305-5164, USA. [2]Department of Microbiology and Immunology, 300 Pasteur Drive, Room D309, Stanford University, Stanford, California 94305, USA. Correspondence should be addressed to M.A.K. (markay@stanford.edu).

Received 21 July 2008; accepted 2 January 2009; published online 1 February 2009; doi:10.1038/nsmb.1552

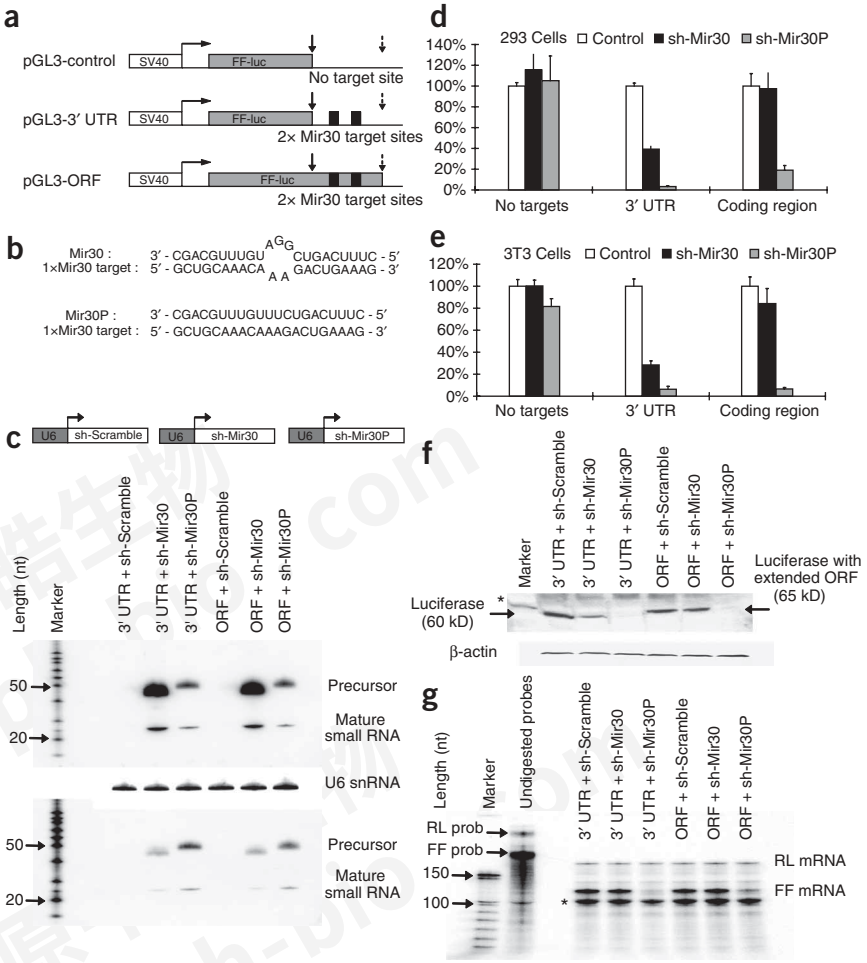

Figure 1 miRNA-mediated repression is abolished in extended ORFs. (**a**) The reporter constructs used in this study. pGL3-control contains no miRNA target sites. pGL3-3′ UTR contains two tandem mir-30 targets sites located in the 3′ UTR. In pGL3-ORF, the upstream stop codon is abolished and the mir-30 target sites are covered by an extended ORF. Grey box represents the ORF of the FF-luciferase gene. Dark boxes represent tandem mir-30 target sites with 6 nt in between. Positions of the upstream (original) stop codon and downstream stop codon are indicated by solid and dotted arrows, respectively. (**b**) Schematic illustration of the interactions between the mir-30 target sequence and the guiding-strand sequence of sh-mir-30 and sh-mir-30P, respectively. (**c**) NIH3T3 cells were co-transfected with plasmids, as described above. Sh-RNA expressed from a U6-driven cassette was detected by northern blotting using either a probe against mir-30 (above) or a probe against mir-30P (below). Owing to sequence similarity, cross-hybridization was observed. Endogenous U6 snRNA was also detected as an internal control. (**d**,**e**) HEK293 cells (**d**) and NIH3T3 cells (**e**) were co-transfected with different combinations of plasmids, and dual-luciferase assays were performed 36 h post-transfection. FF-luciferase activities were normalized with RL-luciferase, and the percentage of relative enzyme activity compared to the negative control (treated with sh-Scramble) was plotted. Error bars represent the s.d. from three independent experiments, each performed in triplicate. (**f**) Protein analysis by western blotting was performed in transfected 3T3 cells. A protein band of β-actin was used as an internal control. Positions of the bands representing wild-type or mutant FF-luciferase were indicated by arrows. A nonspecific band was indicated by an asterisk. (**g**) RNA levels of either FF-luciferase (FF) or RL-luciferase (RL) from transected 3T3 cells were detected by an RNase protection assay. Full-length probes and protected bands are indicated in the figure. A band labeled with an asterisk is possibly due to a truncated RL-luciferase probe and, therefore, corresponds to the RL-luciferase mRNA level.

of the mature miRNA transcripts between transfection experiments (**Fig. 1c**). As expected, co-transfection of HEK293 cells and NIH3T3 cells with plasmids expressing sh-mir-30, sh-mir-30P or a scrambled shRNA with a Firefly luciferase (FF-luciferase) reporter construct without mir-30 target sites did not alter FF-luciferase expression, as measured by enzymatic activity in a dual-luciferase assay (**Fig. 1d**,**e**). Moreover, this experiment established that there were no off-target effects using this reporter system from the U6-shRNA–expressing constructs. Consistent with previous studies[20], sh-mir-30 effectively downregulated FF-luciferase expression by more than 60%, whereas sh-mir-30P inhibited FF-luciferase expression by >90% when tandem mir-30 target sites were present in the 3′ UTR region (**Fig. 1d**,**e**). Notably, when the same target sites were embedded within the extended coding region in both HEK293 cells and NIH3T3 cells (**Fig. 1d**,**e**), sh-mir-30–induced repression, but not sh-mir30P–induced repression, was abolished (<3% for HEK293 cells and <15% for NIH3T3 cells).

The construct containing the tandem mir-30 target sites in the extended ORF was predicted to produce a FF-luciferase with extra amino acids at the C-terminal end. Although the luciferase activity produced from the extended ORF was about 100 times lower than the wild-type FF-luciferase activity (data not shown), the enzymatic activity was still in the linear range of the assay. A western blot showed that, as expected, the ORF-extended protein migrated with a higher molecular weight, with a signal intensity similar to that of the wild-type protein (**Fig. 1f**). Notably, relative changes in the protein-band intensity for both the wild-type and extended ORF paralleled the changes in luciferase-activity measurements under all conditions when they were directly compared.

To confirm that both miRNA- and RNAi-mediated mechanisms were active, we measured luciferase mRNA levels in transfected NIH3T3 cells using an RNase protection assay. Coexpression of the sh-mir-30 and the reporter containing the miRNA target in the 3′ UTR resulted in a 70% downregulation of enzymatic activity and no detectable variation in mRNA, indicating that the reduction in protein level was primarily the result of translational repression, which in turn is suggestive of miRNA-mediated inhibition (**Fig. 1g**). In contrast, the concentration of the FF-luciferase extended ORF mRNA did not change in the presence of mir-30 expression, but was greatly reduced when mir-30P was coexpressed (**Fig. 1g**). These results show that, whereas miRNA-mediated translational inhibition was limited to targets in the untranslated region, RNAi-mediated activity directed against the same sequence remained functional, whether or not the site was within a coding sequence. This is consistent with a previous report[21] where only minor reductions of siRNA-mediated cleavage efficiency were observed when target sites were switched from an untranslated to translated region.

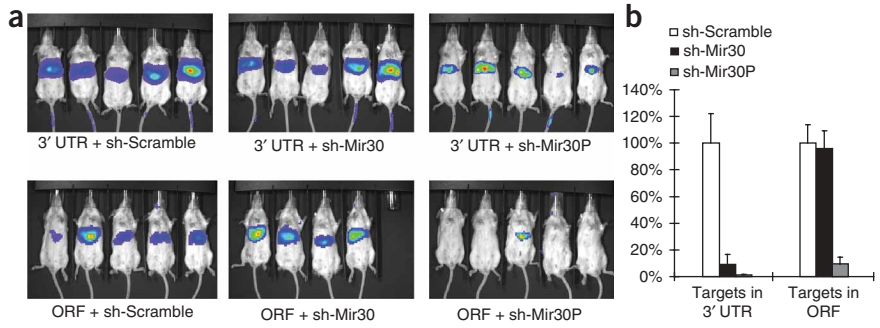

Figure 2 miRNA-mediated repression studies were concordant in mouse liver *in vivo*. (**a**) The plasmids described in **Figure 1** were transfected into mice by hydrodynamic tail injection ($n = 5$ per group, except group 4, where $n = 4$ (one animal died after injection)). Real-time transgene expression was determined 4 d after injection. (**b**) A control plasmid, RSV-hAAT, was co-transfected within each sample as an internal control for transfection efficiency. The FF-luciferase activities were normalized to serum hAAT levels measured by ELISA. The percentage of relative luciferase activity compared to negative controls (treated with sh-Scramble) was plotted. Error bars represent the s.d.

To establish that miRNA-mediated repression between target sites in the 3′ UTR and coding region was not limited to a single reporter system or cell line, we placed the same miRNA targets into an enhanced green fluorescent protein (EGFP) reporter gene and coexpressed this construct with the various miRNAs (**Fig. 1**) in both NIH3T3 (**Supplementary Fig. 1** online) and HEK 293 cells (not shown). These experiments yielded similar results.

As a final test for fidelity, we replaced the mir-30 sequences with a bantam miRNA target. The bantam miRNA was originally identified in *D. melanogaster* and is not believed to have a direct mammalian counterpart[22]. Co-transfection studies using U6-bantam expression plasmids in mammalian cells (**Supplementary Fig. 2a**,**b** online) gave virtually identical results to those observed for the mir-30 constructs in both HEK293 cells and NIH3T3 cells. The ability of the bantam miRNA to repress translation was lost when the target was part of the extended ORF, but the RNAi activity induced by bantam-P was equally robust, whether or not the target was embedded into a coding region (**Supplementary Fig. 2c**,**d**). Moreover, to establish that the accessibility and functionality of the miRNA target were functions of its presence, rather than its specific position, in the 3′ UTR, we varied its location relative to the stop codon and poly(A) signal with the insertion of an irrelevant ~700-bp fragment, and found that this had little effect on miRNA-induced silencing (**Supplementary Fig. 3** online).

ORFs are refractory to miRNA-mediated regulation *in vivo*

To establish that the regulatory miRNA circuit is biologically operative under physiological conditions in whole mammals, we examined the efficiency of the mir-30–luciferase system (**Fig. 1**) in mouse liver. We selected mir-30 because it is not believed to be highly expressed in this tissue[23,24]. Luciferase expression plasmids (**Fig. 1**) were co-transfected into mouse liver via a hydrodynamic tail vein infusion, a method known to transfect up to 30% of mouse hepatocytes *in vivo*[25]. After 4 d, we measured luciferase expression (**Fig. 2a**). To control for variation in transfection efficiencies between individual animals, the FF-luciferase expression data was normalized (**Fig. 2b**) to an added control plasmid expressing a third, unrelated transgene product (Methods).

The data obtained from mouse liver were concordant with the data from tissue-culture cells. Whereas RNAi-mediated knockdown activity was robust whether the target was in the 3′ UTR or part of the extended coding region, miRNA-induced silencing was severely compromised when the target was included within the extended ORF.

Rare codons restore miRNA-mediated knockdown

Because our results suggested that active translation of mRNAs precludes miRNA-induced knockdown, we predicted that ribosome hindrance would interfere with the ability of a miRNA and its associated machinery to attach to its target site. To test this, we introduced a cluster (9 residues) of rare codons upstream of miRNA target sites located in the extended luciferase ORF (**Fig. 3a**), an approach used to cause ribosome pausing in eukaryotes[26,27]. As we could not measure ribosome translocation directly, we constructed several different control sequences for direct comparison. We inserted the same 9 residues in the identical location using an optimized set of codons, or placed the rare codons downstream of the miRNA target. When the rare codons were upstream of the target, miRNA-induced silencing from sh-mir-30 was restored to a level close to that observed for the wild type (rescue of >80% and 70% in HEK293 and NIH3T3 cells, respectively). In contrast, replacing the rare with optimal codons or placing the rare codons downstream of the miRNA target was unable to rescue miRNA-induced silencing (**Fig. 3b–e**). This confirmed that the additional nucleotides or the extra amino acids were not responsible for the differential activity of the miRNA target. To eliminate the possibility that the addition of the extra 27 nucleotides altered the local RNA-folding structure—and, hence, the accessibility and efficacy of miRNA target sites—we inserted these sequences upstream of mir-30 target sites, which remain in the 3′ UTR in the FF-luciferase reporter construct. miRNA-mediated repression was not changed (**Fig. 3f**). RNA analyses confirmed that the rare or optimal codon clusters had no substantial effect on the steady-state mRNA levels (**Fig. 3g**).

To further validate that the rescue of the miRNA repression was due to the brief translational pause mediated by rare codons[26,27], we mapped the accessibility of sequences downstream of the rare and optimal codons using a DNA-oligonuclotide–RNase H approach[28] (**Fig. 4a**). The sequences immediately downstream (~70 nucleotides; **Fig. 4,** Oligos 1–3) of the rare codons were more accessible to RNase H–mediated cleavage than were the same sequences in the mRNAs containing the optimal codons (**Fig. 4b**). In contrast, sequences further downstream of the rare or optimal codons in the 3′ UTR were similar in their accessibility to RNase H cleavage (**Fig. 4a**, Oligos 4 and 5), indicating that the difference in accessibility is specific to the region just downstream of the rare codon tract (**Fig. 4b**). In addition, and consistent with our prediction (**Fig. 4a**), RNase H–mediated cleavage was equal or modestly less robust in sequences contained upstream of the rare versus the optimal codon mRNA sequences, suggesting a slight backup of ribosomes upstream of the rare-codon insertion (**Supplementary Fig. 4** online). As the steady-state production of protein (**Fig. 3e**) and the average density of ribosomes along the mRNA as determined by polysome gradient fractionation (**Supplementary Fig. 5** online) was not substantially altered by the rare-codon insertion, the ribosomal pause during active translation over the specific region covered by oligos 1–3 was likely to be brief.

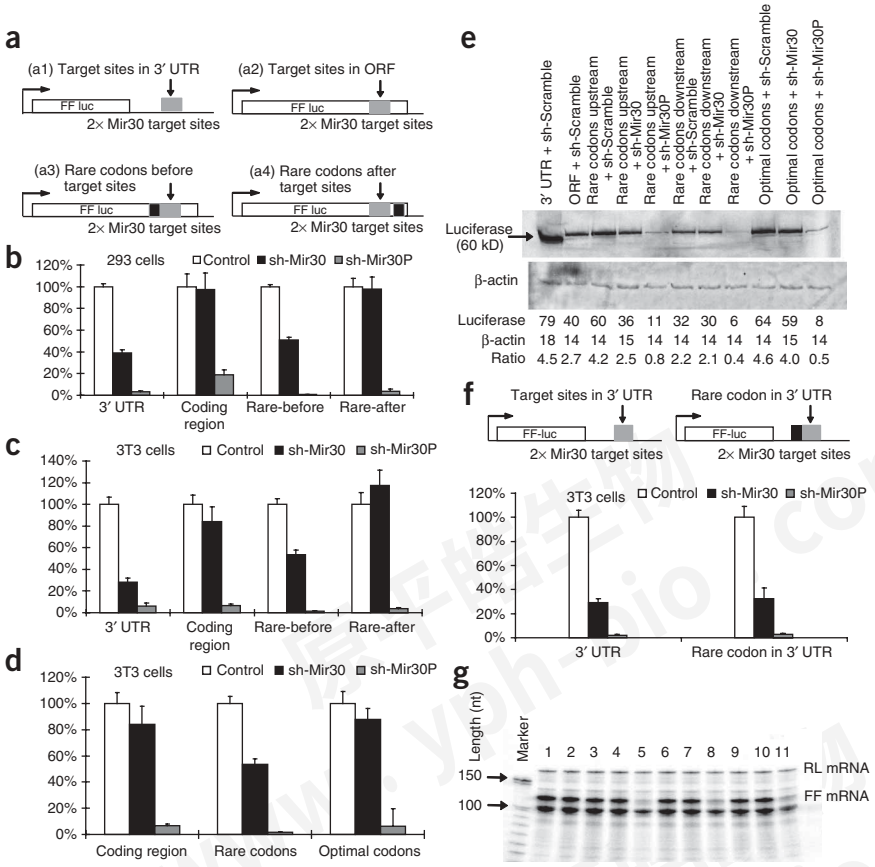

Figure 3 Insertion of rare codons upstream of the extended miRNA ORF rescues miRNA-mediated knockdown. (**a**) The maps of the reporter constructs used in this study. Plasmids containing tandem mir-30 target sequence in either 3′ UTR (a1) or ORF (a2) are the same as those described in **Figure 1**. A cluster of rare codons (represented as a dark box) were inserted either upstream (a3) or downstream (a4) of mir-30 target sequences. In another construct, the upstream rare codons (a3) were replaced with optimal-codon sequences that code for the same peptide sequence. The arrows and gray box represent the position of the miRNA target sequences. (**b**–**d**) HEK293 cells (**d**) and NIH3T3 cells (**c**,**d**) were transfected with the reporter constructs illustrated in **a**. Dual-luciferase assays were performed 36 h post-transfection. FF-luciferase activities were normalized with RL-luciferase, and the percentage of relative enzyme activity compared to the negative control (treated with sh-Scramble) was plotted. Error bars represent s.d. from three independent experiments, each performed in triplicate. (**e**) Protein levels of reporter genes were analyzed by western blotting in transfected NIH3T3 cells. (**f**) NIH3T3 cells were transfected with constructs as indicated in the figure. Insertion of a rare-codon cluster (dark box) upstream of mir-30 targets sites in the 3′ UTR did not substantially change the miRNA-induced repression. (**g**) RNA levels of reporter genes were analyzed by RNase protection assay. The loading sequence of lines 1–11 is same as noted in **e**.

Repressed reporter mRNAs are associated with polyribosomes

Our data were consistent with the requirement of a stable association between miRNA–RISC and target mRNA for miRNA-induced translational repression. We next investigated whether this association results in exclusion of the target mRNA from the translational machinery by analyzing the polysome profiles of repressed target mRNAs. Whole-cell extracts were prepared from NIH3T3 cells transfected with either a luciferase or an EGFP reporter gene containing tandem mir-30 target sequences in either the 3′ UTR or ORF, as well as plasmids expressing sh-mir-30 or sh-Scramble. Polysome-sedimentation profiles of luciferase reporter mRNA and control *Renilla* (RL)-luciferase mRNA were measured by an RNase protection assay (RPA) (**Supplementary Fig. 6** online); EGFP mRNA and actively translated β-actin mRNA levels were determined by northern blotting (**Supplementary Fig. 7** online). Notably, reporter mRNAs containing target sequences in their 3′ UTRs or in the extended ORF and coexpressed with sh-Scramble or sh-mir-30 showed distribution profiles similar to those of actively translated mRNA (RL-luciferase or actin) (**Supplementary Fig. 6b** and **Supplementary Fig. 7a–e**). To establish that these mRNAs were actually associated with polyribosomes, we performed polysome gradient analyses after treatment with puromycin or EDTA, both of which release polysomes. As shown in **Supplementary Figures 6** and **7**, the miRNA-repressed mRNAs shifted to the slow-sedimenting part of the gradient to the same degree as actively

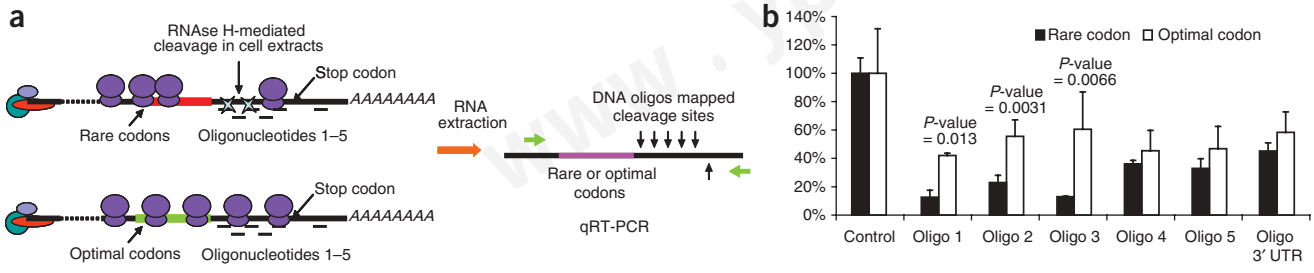

Figure 4 Insertion of rare codons increases the accessibility of downstream sequences to RNase H–mediated cleavage. (**a**) Experimental strategy. Cells were transfected with the luciferase reporter constructs containing the cluster of rare or optimal codons (**Fig. 3a**). After fixing the ribosomes on the mRNA by the addition of cycloheximide, one of six oligonucleotides corresponding to the region between the rare or optimal codons and target 3′ UTR was added into the cell extracts. The hybridization of DNA oligonucleotides at the target site within the mRNA results in cleavage mediated by the endogenous RNase H activity in the cell extracts. The extent of the cleavage represents the relative RNA accessibility, which was quantified by real-time RT-PCR (qRT-PCR) using two primers flanking the cleavage sites. (**b**) Quantification of RNase H–mediated cleavage. The values are presented as the relative PCR signal compared to control samples treated with a scrambled oligonucleotide and normalized for a GFP mRNA obtained from a co-transfected control plasmid.

translated mRNA after puromycin (**Supplementary Figs. 6c** and **7f**,**h**) or EDTA treatment (**Supplementary Figs. 6d** and **7g**,**i**). These results strongly favor a model where miRNA-targeted mRNAs remain associated with the polyribosome. At first consideration, these results seem concordant with some studies[29–33] but contrast with other studies where miRNA-repressed mRNAs were found in the fast-sedimenting[34,35] or puromycin-resistant, slow-sedimenting pseudo-polysomal fractions[36].

DISCUSSION

Taken together, our studies, using multiple expression systems, cells and miRNA targets, are in good concordance. Although our results suggest that location within the 3′ UTR may not cause a large functional difference, there does seem to be a functional reason for the localization of miRNA targets in the 3′ UTR. We propose that these functional constraints may be the primary explanation for the observed distribution pattern of miRNA targets found in mammalian cells. However, other studies have reported that artificially designed, mismatched siRNA or shRNA co-delivery studies can result in some translational repression when mRNAs contained target sequences in the coding regions[37,38]. The source of these contradictions is not completely clear, but in several studies the mismatched synthetic siRNAs were provided in very high concentrations. Other factors possibly contributing to the degree of repression between miRNAs and their corresponding targets may include sequence composition[4], number of target sites[39], local RNA structure[40] and distance between target sites[41]. Adding or removing miRNA target sites in coding regions may not elucidate the true natural functional differences between a target site residing in the coding region and one residing in the 3′ UTR. In our study, we carefully designed our reporter constructs such that there was only one nucleotide difference between the mRNA sequences that we compared directly. Therefore, the reduction of miRNA-induced gene repression should be a direct result of changing the target location from the 3′ UTR to the ORF without making major alterations in the mRNA sequence.

Our data support a model whereby miRNA-programmed RISC is required to remain attached to the target mRNA to effectively silence translation *in cis*. Moreover, when target sites remain at the same site in the mRNA but become part of the coding region, we suggest that ribosomal complexes override and inhibit the miRNA-programmed RISC from attaching to the target site. If the translational process is slowed, we speculate that there is less physical constraint by the ribosomes, thus allowing miRNA-programmed RISC to attach to the target.

This process seems to be functionally distinct from RISC RNAi-mediated RNA degradation, because converting the miRNA to give it perfect complementarity to the target still resulted in loss of the mRNA, presumably through the RNAi pathway, whether the miRNA target was part of the extended coding sequence or located in the 3′ UTR. This is consistent with the finding that, unlike in mammals, miRNA target sites in plants are widely distributed across coding regions, as nearly all of them have perfect complementarity with their target sequences and function through an RNAi-mediated degradation pathway. Curiously, the only known mammalian miRNA that targets the coding region in the mRNA has perfect complementarity with its targets and also functions through RISC-mediated cleavage[42]. Nonetheless, we cannot exclude the possibility that some functional miRNA targets exist in coding regions. If such sites are identified, it will be of great interest to determine whether they are preceded by rare codons. In fact, one study provided evidence for a functional miRNA target in the coding region of an endogenous mammalian gene[43]. The mRNA was active when it had an extensive 17-bp, but not the more classical, 7-bp, 5′ seed match with the mRNA sequence. This suggests that the downregulation may have been mediated by RNAi cleavage rather than by translational downregulation[44].

It will also be of interest in future studies to determine when functional miRISC–mRNA complexes can be assembled in the post-transcriptional life of an mRNA . Our results show that, if translocation of the ribosome is slow, miRISC complexes can still form after translational initiation begins. We favor a model where miRNA–RISC binding to actively translating mRNAs results in reduced translational elongation and termination, concordant with a reduction in ribosomal initiation and possible nascent-peptide destabilization[32,33].

Here we provide evidence for why endogenous miRNA target sites are found in noncoding regions, but it is also logical to ask why relatively few miRNA targets are localized in the 5′ UTR. When the translation-initiation complex forms around the cap structure, the 40S subunit of the ribosome will scan the 5′ UTR until it identifies the first AUG sequence, where the 60S subunit joins to form an 80S ribosome. It is possible that the scanning process impairs the formation of miRNA–RISC complexes in some 5′ UTRs, depending on its structure, which can be complex. Our preliminary studies were consistent with this, because we found a great degree of discordance between different miRNA-target 5′ UTR insertions and the degree of translational repression (S.G. and M.A.K., unpublished data). Nonetheless, there are examples of miRNAs that do function with 5′ UTR targets. Whereas one study shows that the mir-122 target sites located in the 5′ UTR region of the hepatitis C virus are important to maintain robust viral replication[45], another reports that the mRNA-bearing miRNA target sites in the 5′ UTR can be repressed as effectively as those having miRNA target sites in the 3′ UTR[46]. Further studies are needed to establish the extent to which functional miRNA targets are present in these noncoding regions.

METHODS

Plasmid constructions. Both strands of 2×Mir30 target sites were chemically synthesized (sense strand: 5′-AATTCGCTGCAAACAAAGACTGAAAGAACT AGTGCGCTGCAAACAAAGACTGAAAGCTGCA-3′; antisense strand 5′-GCTTTCAGTCTTTGTTTGCAGCGCACTAGTTCTTTCAGTCTTTGTTTGCA GCG-3′), annealed, purified and inserted between EcoRI and PstI sites 67 bp downstream of the FF-luciferase coding region in a pGL3 construct with modified 3′ UTR sequences. We used PCR-based point-mutagenesis approaches to create a single-point insertion to disrupt the stop codon of the FF-luciferase gene. A similar approach was used to generate the GFP reporter system and the FF-luciferase reporter system with bantam target sequences. An ~700-bp sequence in the middle of a kanamycin-resistance gene–coding region was PCR amplified and then inserted into various cloning sites upstream or downstream of the miRNA target sites to reposition the miRNA targets within different regions of the 3′ UTR.

Rare codon sequences (5′-GCG CCG GTA ACG GTA CCG GCG ACG GCG-3′) or optimal codon sequences (5′-GCC CCC GTC ACC GTC CCC GCC ACC GCC-3′) were inserted either 53 bp upstream or immediately downstream of the mir-30 target sites. Mir-30/mir-30P or bantam/bantam-P shRNAs were designed as a passenger strand, followed by the mir-22 loop sequence (5′-CCTGACCCA-3′), followed by the guiding-strand sequence. These were cloned downstream of the U6 ploymerase III promoter.

Cell culture and transfections. Adherent HEK293 and NIH3T3 cells were grown in DMEM (Gibco-BRL) with 2 mM L-glutamine and 10% (v/v) heat-inactivated FBS with antibiotics. All transfection assays were done using Lipofectamine 2000 (Invitrogen) following the manufacturer's protocol. HEK293 and NIH3T3 cells at 90% confluency were transfected in 24-well plates with 50 ng FF-luciferase or EGFP reporter DNA, 50 ng shRNA expression DNA and 5 ng RL-luciferase DNA, unless specified otherwise. Unless indicated, cells were assayed 36 h after transfection.

Dual-luciferase assay. FF-luciferase and RL-luciferase were measured using Promega's dual-luciferase kit (catatalg no. E1980) protocol and detected by a Modulus Microplate Luminometer (Turner BioSystems).

Western blots. NIH3T3 cells (36 h after transfection) were lysed with mammalian protein-extraction reagent from M-PER (PIERCE, catalog no. 78501) with protease inhibitors (Roche, catalog no. 11836153001). The samples were denatured in Laemmli sample buffer (Bio-RAD, catalog no. 161-0737) for 5 min at 95 °C and separated in 10% (w/v) SDS-PAGE gels. The denatured proteins were then electrotransferred onto a PVDF membrane blocked with 5% (w/v) fat-free milk powder in PBS and 0.5% (v/v) Tween 20 for 1 h. Either an anti–FF-luciferase antibody (diluted 1:5,000, Abcam), anti-GFP antibody (diluted 1:1,000, Abcam) or anti–β-actin antibody (diluted 1:8,000, Sigma) was used. Following three washes in PBS for 5 min, a secondary antibody (horseradish peroxidase (HRP)–anti-mouse IgG; diluted 1:10,000, Sigma) was added for 1 h at room temperature (25 °C), followed by three 5-min washes in PBS. Antibody-bound proteins were visualized using the ECL western blotting analysis system (Amersham, RPN2109).

Northern blots and RNase protection assay. Total RNA was isolated using Trizol (Invitrogen). The DNA-free kit (Ambion, catalog no. 1906) was used to purify total RNA from contaminating DNAs. Total RNA (10–20 μg) was electrophoresed on 1% (w/v) agarose gel. After transfer onto Hybond-N1 membrane (Amersham Pharmacia Biotech), target mRNAs were detected using P32-labeled full-length cDNA probes.

RPA assays were carried out using the Ambion PRA III kit (catalog no. AM1414). P32-labeled antisense RNA probes against either FF-luciferase or RL-luciferase were generated by *in vitro* transcription (Ambion MAXIscript Kit, catalog no. AM1308). DNA templates were produced by PCR using primer sets (FF-luc: 5′-ATCCATCTTGCTCCAACACC-3′ and 5′-TTTTCCGTCATCGTCT TTCC-3′; RL-luc: 5′-GATAACTGGTCCGCAGTGGT-3′ and 5′-ATTTGCCTGA TTTGCCCATA-3′). Total RNA from NIH3T3 cells was isolated by Trizol (Invitrogen) 36 h after transfection and purified using a DNA-free kit (Ambion, catalog no.1906). Hybridization reactions were carried out at 55 °C overnight and RNase digestion at 37 °C for 30 min using the RNase A/T1 cocktail provided in the RPA III kit.

Hydrodynamic tail injection and luciferase imaging. Animals studies were done in concordance with the US National Institutes of Health guidelines and the Stanford Animal Care Committee. Female BALB/c mice, 6–8 weeks of age (Jackson Laboratory) were hydrodynamically infused with a mixture of 2 μg FF-luciferase DNA, 2 μg of the appropriate shRNA plasmid, 2 μg of an RSV-hAAT expression cassette DNA and 34 μg pBluescript plasmid DNA (Stratagene), and were then imaged for luciferase. As described[47], raw light values were reported as relative detected light photons per minute, and normalized for serum hAAT expression.

Polyribosome fractionation. Polysomal mRNA was prepared based on a method described previously[48]. Briefly, before being harvested, cells were incubated with 0.1 mg ml^{-1} cycloheximide for 3 min at 37 °C. NIH3T3 cells were harvested directly on their culture dish in lysis buffer (15 mM Tris-HCl, pH 7.4, 15 mM $MgCl_2$, 0.3 M NaCl, 1% (v/v) Triton X-100, 0.1 mg ml^{-1} cycloheximide and 1 mg ml^{-1} heparin) and loaded onto 10–50% (w/v) sucrose gradients composed of the same extraction buffer lacking Triton X-100. The gradients were sedimented at 210,000*g* (max.) for 180 min in a SW41 rotor at 4 °C. Fractions of equal volumes were collected from the top using an ISCO fraction-collector system. RNAs were extracted by phenol-chloroform followed by isopropanol precipitation, washes in 75% (v/v) ethanol and resuspension in DNase I reaction buffer (Turbo DNase, Ambion).

Mapping accessibility. This approach is modified from a previous publication[49]. HEK293 cells were transfected with plasmids expressing the FF-luciferase reporter gene embedded with the cluster of rare or optimal codons along with a GFP control plasmid. At 36 h post-transfection, cells were harvested after incubation with 0.1 mg ml^{-1} cycloheximide for 3 min at 37 °C. After three washes with PBS, approximately 2×10^7 cells were pelleted and resuspended in two times the volume of the cell pellet in hypotonic swelling buffer (7 mM Tris-HCl, pH7.5, 7 mM KCl, 1 mM MgCl2 and 1 mM β-mercaptoethanol). After a 10-min incubation on ice, samples were Dounce homogenized (VWR) 40 times with a tight pestle B followed by addition of one-tenth of the final volume of neutralizing buffer (21 mM Tris-HCl, pH 7.5, 116 mM KCl, 3.6 mM MgCl2 and 6 mM β-mercaptoethanol). After centrifugation of the homogenates at 20,000*g* for 10 min at 4 °C, the supernatants were collected. The RNase H–mediated–cleavage experiments were carried out in a total volume of 300 μl, containing 280 μl cell extracts, 1 mM DTT, 20–40 units RNase inhibitor (Promega) and 50 nM each of the defined sequence antisense deoxyribooligonucleotides (ODNs) (**Supplementary Table 1** online). The ODNs were incubated in the extracts for 5 min at 37 °C. Total RNA was extracted by phenol-chloroform extraction. After the reverse transcription reaction (Invitrogen RT kit, catalog no. 18080-051) with oligo dT primer, real-time PCR (Qiagen, QuantiTect SYBR green PCR kit) was performed with two primers flanking the cleavage sites. (Upstream: 5′-AGGCCAAGAAGGGCGGAAAG-3′ or 5′-ACCGCGAAAAAGTTGCGCG-3′; downstream: 5′-TCACTGCATTC TAGTTGTGG-3′). All results are obtained with $R > 0.98$). Each oligonucleotide was tested six times in two separate experiments. *P*-values were calculated using the Student's *t*-test.

Note: Supplementary information is available on the Nature Structural & Molecular Biology website.

ACKNOWLEDGMENTS

This work was supported by the US National Institutes of Health grant DK 78424. We thank B. Hu for helping prepare some of the samples, R. Cevailos for technical assistance with the polyribosome fractionation experiments and D. Haussecker for critical reading of the manuscript.

AUTHOR CONTRIBUTIONS

S.G. designed and implemented most of the experiments; L.J. performed the studies outlined in **Figure 4**; F.Z. assisted S.G. with the molecular biology preparations; P.S. provided assistance with the polysome studies and offered critical discussions related to data interpretation; M.A.K. supervised the studies and provided scientific input into the experimental design and data interpretation; S.G and M.A.K wrote the manuscript; all authors approved the final manuscript.

Published online at http://www.nature.com/nsmb/
Reprints and permissions information is available online at http://npg.nature.com/reprintsandpermissions/

1. Ambros, V. The functions of animal microRNAs. *Nature* **431**, 350–355 (2004).
2. Bartel, D.P. MicroRNAs: genomics, biogenesis, mechanism, and function. *Cell* **116**, 281–297 (2004).
3. Berezikov, E. *et al.* Phylogenetic shadowing and computational identification of human microRNA genes. *Cell* **120**, 21–24 (2005).
4. Lewis, B.P., Burge, C.B. & Bartel, D.P. Conserved seed pairing, often flanked by adenosines, indicates that thousands of human genes are microRNA targets. *Cell* **120**, 15–20 (2005).
5. Xie, X. *et al.* Systematic discovery of regulatory motifs in human promoters and 3′ UTRs by comparison of several mammals. *Nature* **434**, 338–345 (2005).
6. O'Donnell, K.A., Wentzel, E.A., Zeller, K.I., Dang, C.V. & Mendell, J.T. c-Myc-regulated microRNAs modulate E2F1 expression. *Nature* **435**, 839–843 (2005).
7. He, L. *et al.* A microRNA polycistron as a potential human oncogene. *Nature* **435**, 828–833 (2005).
8. Triboulet, R. *et al.* Suppression of microRNA-silencing pathway by HIV-1 during virus replication. *Science* **315**, 1579–1582 (2007).
9. Vaucheret, H. Post-transcriptional small RNA pathways in plants: mechanisms and regulations. *Genes Dev.* **20**, 759–771 (2006).
10. Lai, E.C. Micro RNAs are complementary to 3′ UTR sequence motifs that mediate negative post-transcriptional regulation. *Nat. Genet.* **30**, 363–364 (2002).
11. Lewis, B.P., Shih, I.H., Jones-Rhoades, M.W., Bartel, D.P. & Burge, C.B. Prediction of mammalian microRNA targets. *Cell* **115**, 787–798 (2003).
12. Doench, J.G. & Sharp, P.A. Specificity of microRNA target selection in translational repression. *Genes Dev.* **18**, 504–511 (2004).
13. Meister, G. *et al.* Human Argonaute2 mediates RNA cleavage targeted by miRNAs and siRNAs. *Mol. Cell* **15**, 185–197 (2004).
14. Liu, J. *et al.* Argonaute2 is the catalytic engine of mammalian RNAi. *Science* **305**, 1437–1441 (2004).
15. Pillai, R.S., Bhattacharyya, S.N. & Filipowicz, W. Repression of protein synthesis by miRNAs: how many mechanisms? *Trends Cell Biol.* **17**, 118–126 (2007).
16. Valencia-Sanchez, M.A., Liu, J., Hannon, G.J. & Parker, R. Control of translation and mRNA degradation by miRNAs and siRNAs. *Genes Dev.* **20**, 515–524 (2006).

17. Liu, J., Valencia-Sanchez, M.A., Hannon, G.J. & Parker, R. MicroRNA-dependent localization of targeted mRNAs to mammalian P-bodies. *Nat. Cell Biol.* **7**, 719–723 (2005).
18. Sen, G.L. & Blau, H.M. Argonaute 2/RISC resides in sites of mammalian mRNA decay known as cytoplasmic bodies. *Nat. Cell Biol.* **7**, 633–636 (2005).
19. Bagga, S. *et al.* Regulation by let-7 and lin-4 miRNAs results in target mRNA degradation. *Cell* **122**, 553–563 (2005).
20. Zeng, Y., Wagner, E.J. & Cullen, B.R. Both natural and designed micro RNAs can inhibit the expression of cognate mRNAs when expressed in human cells. *Mol. Cell* **9**, 1327–1333 (2002).
21. Gu, S. & Rossi, J.J. Uncoupling of RNAi from active translation in mammalian cells. *RNA* **11**, 38–44 (2005).
22. Brennecke, J., Hipfner, D.R., Stark, A., Russell, R.B. & Cohen, S.M. *bantam* encodes a developmentally regulated microRNA that controls cell proliferation and regulates the proapoptotic gene *hid* in *Drosophila*. *Cell* **113**, 25–36 (2003).
23. Lagos-Quintana, M. *et al.* Identification of tissue-specific microRNAs from mouse. *Curr. Biol.* **12**, 735–739 (2002).
24. Takada, S. *et al.* Mouse microRNA profiles determined with a new and sensitive cloning method. *Nucleic Acids Res.* **34**, e115 (2006).
25. Yant, S.R. *et al.* Somatic integration and long-term transgene expression in normal and haemophilic mice using a DNA transposon system. *Nat. Genet.* **25**, 35–41 (2000).
26. Fernandez, J. *et al.* Ribosome stalling regulates IRES-mediated translation in eukaryotes, a parallel to prokaryotic attenuation. *Mol. Cell* **17**, 405–416 (2005).
27. Lemm, I. & Ross, J. Regulation of c-myc mRNA decay by translational pausing in a coding region instability determinant. *Mol. Cell. Biol.* **22**, 3959–3969 (2002).
28. Scherr, M. *et al.* Detection of antisense and ribozyme accessible sites on native mRNAs: application to NCOA3 mRNA. *Mol. Ther.* **4**, 454–460 (2001).
29. Seggerson, K., Tang, L. & Moss, E.G. Two genetic circuits repress the *Caenorhabditis elegans* heterochronic gene *lin-28* after translation initiation. *Dev. Biol.* **243**, 215–225 (2002).
30. Olsen, P.H. & Ambros, V. The *lin-4* regulatory RNA controls developmental timing in *Caenorhabditis elegans* by blocking LIN-14 protein synthesis after the initiation of translation. *Dev. Biol.* **216**, 671–680 (1999).
31. Maroney, P.A., Yu, Y., Fisher, J. & Nilsen, T.W. Evidence that microRNAs are associated with translating messenger RNAs in human cells. *Nat. Struct. Mol. Biol.* **13**, 1102–1107 (2006).
32. Nottrott, S., Simard, M.J. & Richter, J.D. Human let-7a miRNA blocks protein production on actively translating polyribosomes. *Nat. Struct. Mol. Biol.* **13**, 1108–1114 (2006).
33. Petersen, C.P., Bordeleau, M.E., Pelletier, J. & Sharp, P.A. Short RNAs repress translation after initiation in mammalian cells. *Mol. Cell* **21**, 533–542 (2006).
34. Bhattacharyya, S.N., Habermacher, R., Martine, U., Closs, E.I. & Filipowicz, W. Relief of microRNA-mediated translational repression in human cells subjected to stress. *Cell* **125**, 1111–1124 (2006).
35. Pillai, R.S. *et al.* Inhibition of translational initiation by Let-7 MicroRNA in human cells. *Science* **309**, 1573–1576 (2005).
36. Thermann, R. & Hentze, M.W. *Drosophila* miR2 induces pseudo-polysomes and inhibits translation initiation. *Nature* **447**, 875–878 (2007).
37. Saxena, S., Jonsson, Z.O. & Dutta, A. Small RNAs with imperfect match to endogenous mRNA repress translation. Implications for off-target activity of small inhibitory RNA in mammalian cells. *J. Biol. Chem.* **278**, 44312–44319 (2003).
38. Kloosterman, W.P., Wienholds, E., Ketting, R.F. & Plasterk, R.H. Substrate requirements for let-7 function in the developing zebrafish embryo. *Nucleic Acids Res.* **32**, 6284–6291 (2004).
39. Doench, J.G., Petersen, C.P. & Sharp, P.A. siRNAs can function as miRNAs. *Genes Dev.* **17**, 438–442 (2003).
40. Long, D. *et al.* Potent effect of target structure on microRNA function. *Nat. Struct. Mol. Biol.* **14**, 287–294 (2007).
41. Saetrom, P. *et al.* Distance constraints between microRNA target sites dictate efficacy and cooperativity. *Nucleic Acids Res.* **35**, 2333–2342 (2007).
42. Yekta, S., Shih, I.H. & Bartel, D.P. MicroRNA-directed cleavage of HOXB8 mRNA. *Science* **304**, 594–596 (2004).
43. Duursma, A.M., Kedde, M., Schrier, M., le Sage, C. & Agami, R. miR-148 targets human DNMT3b protein coding region. *RNA* **14**, 872–877 (2008).
44. Hutvagner, G. & Zamore, P.D. A microRNA in a multiple-turnover RNAi enzyme complex. *Science* **297**, 2056–2060 (2002).
45. Jopling, C.L., Yi, M., Lancaster, A.M., Lemon, S.M. & Sarnow, P. Modulation of hepatitis C virus RNA abundance by a liver-specific MicroRNA. *Science* **309**, 1577–1581 (2005).
46. Lytle, J.R., Yario, T.A. & Steitz, J.A. Target mRNAs are repressed as efficiently by microRNA-binding sites in the 5′ UTR as in the 3′ UTR. *Proc. Natl. Acad. Sci. USA* **104**, 9667–9672 (2007).
47. Grimm, D. *et al.* Fatality in mice due to oversaturation of cellular microRNA/short hairpin RNA pathways. *Nature* **441**, 537–541 (2006).
48. Johannes, G. & Sarnow, P. Cap-independent polysomal association of natural mRNAs encoding c-myc, BiP, and eIF4G conferred by internal ribosome entry sites. *RNA* **4**, 1500–1513 (1998).
49. Gu, S., Ji, J., Kim, J.D., Yee, J.K. & Rossi, J.J. Inhibition of infectious human immunodeficiency virus type 1 virions via lentiviral vector encoded short antisense RNAs. *Oligonucleotides* **16**, 287–295 (2006).